

Article

Specialized Olefin Metathesis Catalysts Featuring Unsymmetrical *N*-Heterocyclic Carbene Ligands Bearing *N*-(Fluoren-9-yl) Arm

Phillip I. Jolly, Anna Marczyk, Paweł Małecki, Damian Trzybiński, Krzysztof Woźniak , Anna Kajetanowicz * and Karol Grela *

Biological and Chemical Research Centre, Faculty of Chemistry, University of Warsaw, Żwirki i Wigury Street 101, 02-089 Warsaw, Poland; drphillipjolly@hotmail.com (P.I.J.); a.marczyk@chem.uw.edu.pl (A.M.);

pawelmalecki.chem@gmail.com (P.M.); dtrzybinski@cnbc.uw.edu.pl (D.T.); kwozniak@chem.uw.edu.pl (K.W.)

* Correspondence: a.kajetanowicz@uw.edu.pl (A.K.); prof.grela@gmail.com (K.G.)

Received: 4 May 2020; Accepted: 24 May 2020; Published: 27 May 2020



Abstract: Beneficial structural motifs from two known state-of-the-art olefin metathesis catalysts types, bearing unsymmetrical *N*-heterocyclic carbenes (uNHCs), were combined into a new hybridized design thereby translating the complementary beneficial reactivity demonstrated by their ‘parent’ complexes to the new *N*-fluorene derived olefin metathesis catalysts. Two chelating 2-iso-propoxy-benzylidene (Hoveyda-type) and two 3-phenyl-1*H*-inden-1-ylidene (indenylidene-type) complexes were successfully prepared by in situ generation of either the *N*’-mesityl (Mes) or *N*’-diisopropylphenyl (Dipp) derived uNHCs taking advantage of the thermal decomposition of the corresponding 2-(penta-fluorophenyl)-imidazolidines (NHC adducts). The new fluorene-derived catalysts mediate challenging olefin metathesis processes, such as α -olefin self-metathesis, with high selectivity and conversion.

Keywords: homogeneous catalysis; olefin metathesis; ruthenium; *N*-heterocyclic carbenes; selectivity; ethenolysis

1. Introduction

Formation of a carbon–carbon double bond can be accomplished by various chemical reactions, and catalytic olefin metathesis [1,2] is not only one of the most recent, but also goes well in line with the principles of so-called “green chemistry” [3]. The main driving force behind its development was the introduction of well-defined, active, and water stable Ru catalysts [4,5]. The development of second generation complexes [6–8] by replacement of one of the phosphine ligands with *N*-heterocyclic carbene (NHC) ligands represents a significant landmark in catalyst design, affording both enhanced activity and stability (Figure 1a) [7]. While these “general-purpose” catalysts dominate olefin metathesis, for some niche applications more specialized catalysts bearing unsymmetrical NHC ligands (uNHC) have been introduced. These catalysts were recently reviewed [9,10]; thus, only a few historically representative chemical structures are presented in Figures 1b and 2.

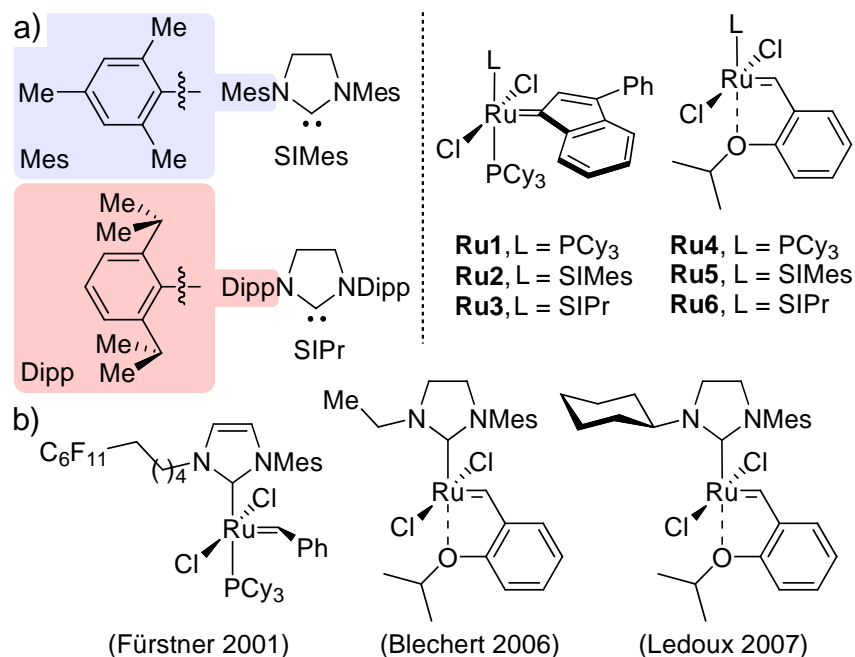


Figure 1. (a) Popular symmetrical *N*-heterocyclic carbene (NHC) ligands and selected general purpose Ru metathesis catalysts (**Ru1–Ru6**). (b) Selected representative Ru complexes containing unsymmetrical NHC ligands.

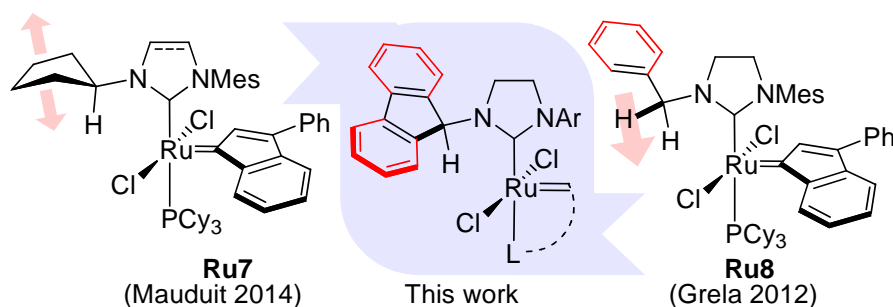
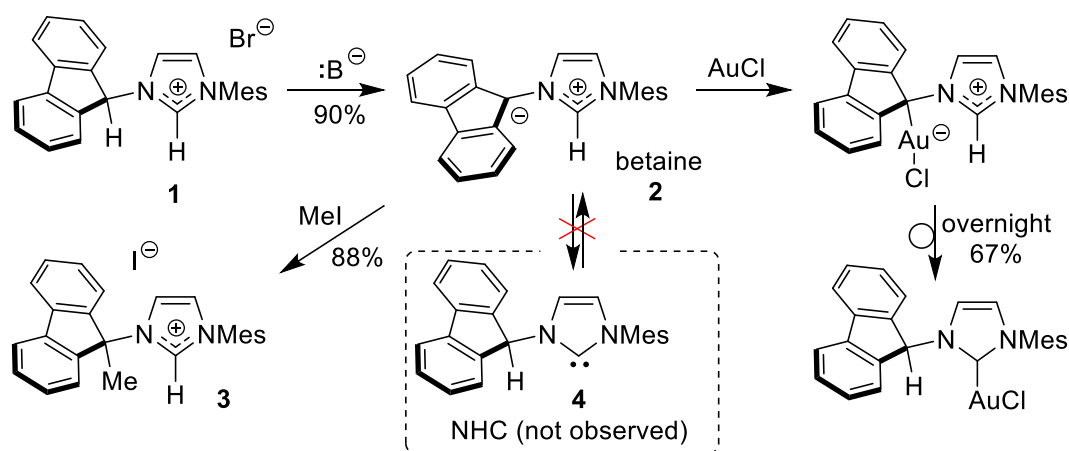


Figure 2. Combined structural characteristics leading to development of a new system (the arrows symbolize the direction of the planned steric enlargement).

The first representatives of this new class of complexes were Grubbs-type uNHC catalysts obtained by Fürstner [11], before the Hoveyda-type complexes were synthesized by Blechert [12] and soon after by Verpoort and Ledoux [13]. Since then, the development of ruthenium catalysts bearing uNHC ligands has continued, however at a significantly slower pace as compared with a fast growing family of symmetrical NHC–Ru complexes [14,15]. This situation can be seen as disadvantageous, as uNHC-catalysts have shown enhanced application profiles in some specialized, but challenging, metathesis applications such as industrially important ethenolysis [16–20], self-metathesis of α -olefins [21,22], and other challenging transformations [23]. Indeed, the replacement of symmetrical NHC ligands with their unsymmetrical counterparts, in particular those with sterically differentiated substituents on nitrogen atoms, significantly increases the stability of resulting complexes in ethylene atmosphere and at higher temperatures [16,21,22,24–27]. This inhibits the formation of catalyst decomposition products which are known to promote the undesirable double bond migrations, and thus increases the yield and selectivity of the process [28–30]. Enhanced stability, especially under harsh conditions, has proven to be beneficial for macrocyclization reactions performed at high concentration [27]. Based on the successful design by Mauduit (**Ru7**) [21] and on the catalyst obtained previously by us (**Ru8**) [22,25,31], we decided to combine the selected structural characteristics of these complexes into a new system bearing an *N*-(fluoren-9-yl) side-arm (Figure 2). We speculated that formal addition of two benzene rings fused into a cyclopentene

ring of Mauduit's **Ru7** [21,32] will increase the steric bulk and produce substantial stiffness around this portion of the complex. Similarly, the fluorenyl substituent can be seen as the enlarged version of the NHC ligand present in **Ru8** [25,31,33].

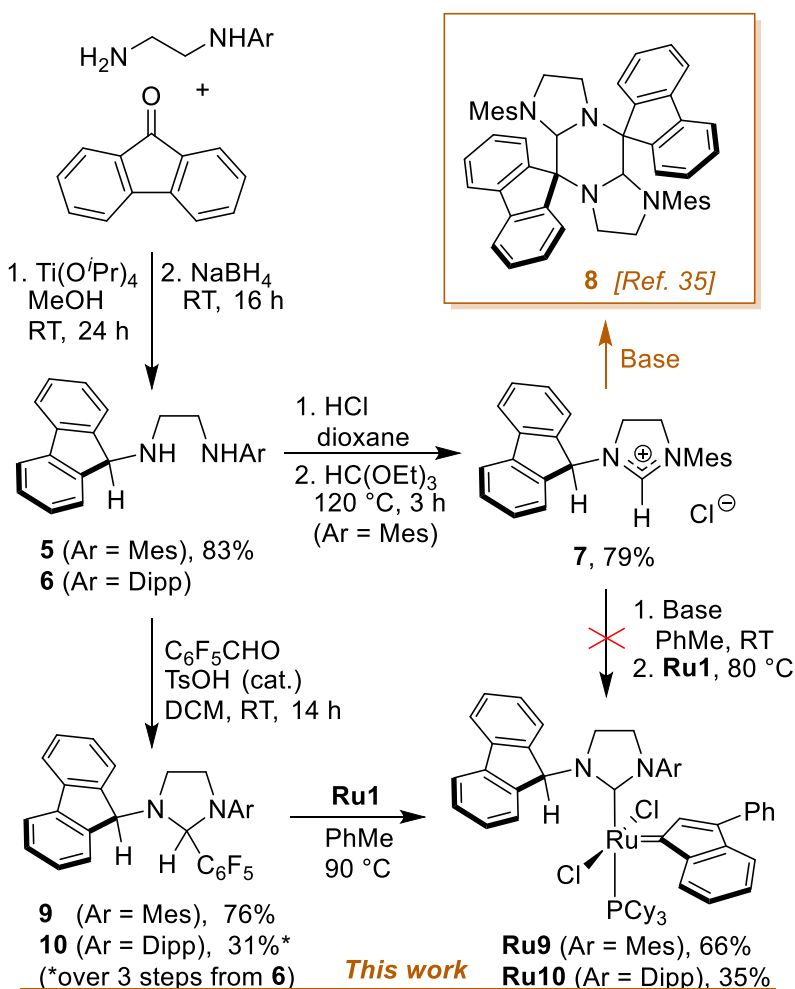
Lavigne and César previously studied aromatic 1-mesityl-3-(fluoren-9-yl)imidazolium salt **1** (Scheme 1) [34]. Interestingly, deprotonation of **1** with strong base did not lead to a corresponding free *N*-(fluoren-9-yl)-imidazol-2-ylidene NHC **4** but to the mesomeric *N*-ylide betaine **2**, consisting of a fluorenyl anion directly attached to an imidazolium ring. This product does not exist in equilibrium with a free NHC tautomer, and upon the reaction with gold and rhodium salts the fluorenyl position is metallated exclusively, not the apparently non-existent carbenic center. Moreover, the pronounced ylidic character of betaine **2** was proven by its reaction with electrophiles, such as methyl iodide, leading to fully selective methylation at the fluorenyl position to yield cleanly the imidazolium iodide **3** (Scheme 1).



Scheme 1. Formation of mesomeric betaine **2** instead of free carbene **4** in deprotonation reaction of 1-mesityl-3-(fluoren-9-yl) imidazolium bromide (**1**), as reported by Lavigne and César [34].

2. Results and Discussion

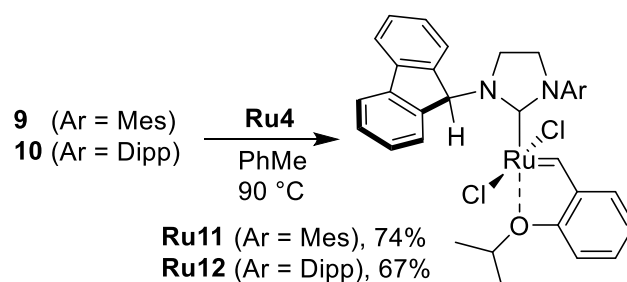
The results reported by Lavigne and César [34] (Scheme 1) were not surprising for us, as we expected that the reactivity of a fluorene-substituted NHC can be very different than the one exhibited by standard SIMes or SIPr (see Scheme 2 for definitions) carbenes. Indeed, in our preliminary work [35], we observed that corresponding (saturated) imidazolinium salt **7** treated with base and ruthenium complex **Ru1** did not lead to even traces of the expected Ru–NHC complex **Ru9** (Scheme 2). Eventually, a solution to that problem was proposed [35], but because in our previous work we focused on studying the ylidic character of the deprotonated **7** and products of its further reactions (such as dimer **8**, Scheme 1), the use of **7** for preparation of Ru metathesis catalysts was signaled only but not explored in detail [35]. Thus, applications of **Ru9** in catalytic olefin metathesis remained generally unknown. In the present work, we describe the synthesis, characterization, and a detailed catalytic activity screening of this complex along with three new derivatives.



Scheme 2. Synthesis of Ru indenylidene complexes bearing *N*-(fluoren-9-yl) substituted NHC ligands with *N'*-mesityl (Mes) or *N'*-diisopropylphenyl (Dipp) (this work) *N*-aryl wings, versus the previously reported azolinium **7** and deprotonation product **8** [35].

As no desired complex formation was observed via direct deprotonation of azolinium salt and reaction with **Ru1**, the catalysts were prepared in good yields by generating the base sensitive fluorene derived uNHCs via thermal disproportionation of 2-(pentafluorophenyl)imidazolidines (**9**) and **10** in the presence of **Ru1** (Scheme 2). To do so, pentafluorophenyl adducts of NHC precursors were prepared in a three-step procedure (for use of pentafluorophenyl adducts in olefin metathesis catalyst synthesis see [25,36,37]). First, condensation of the corresponding *N*-arylethane-1, 2-diamine, and fluorenone was performed, followed by reduction with sodium borohydride. A further condensation of diamines **5** and **6** with pentafluorobenzaldehyde afforded the desired products **9** and **10** with moderate to good yield. Next, the corresponding second-generation indenylidene-type complexes **Ru9** and **Ru10** were obtained in 66% and 35% yield via the in situ generation of free NHC carbenes in the presence of indenylidene first-generation catalyst.

In a similar way, two fluorenyl-NHC Hoveyda-type complexes were obtained (Scheme 3). The preparation was even more efficient, allowing the synthesis of compounds **Ru11** and **Ru12** in improved yields of 67% and 74%, respectively.



Scheme 3. Synthesis of Hoveyda-type complexes bearing *N*-(fluoren-9-yl) substituted NHC ligands.

The identity of **Ru9–Ru12** was unambiguously characterized by single-crystal X-ray diffraction analysis (Figure 3). The investigated compounds crystallized in the orthorhombic $P2_12_12_1$ (**Ru9** and **Ru10**) or $Pbc2_1$ (**Ru11**) and monoclinic $P2_1/c$ space groups (**Ru12**) with one (**Ru9**, **Ru10**, and **Ru12**) and two molecules (**Ru11**) of a given compound in the asymmetric part of the unit cell (Figure S1 in Supplementary Materials). The asymmetric parts of **Ru10** and **Ru12** also contain molecules of solvents (Figure S1). The values of selected parameters describing the geometry of molecules of **Ru9–Ru12** are given in Table 1, while the details of crystallographic data and refinement parameters as well as a full list of bond lengths and values of valence and torsion angles are summarized in Tables S7–S18.

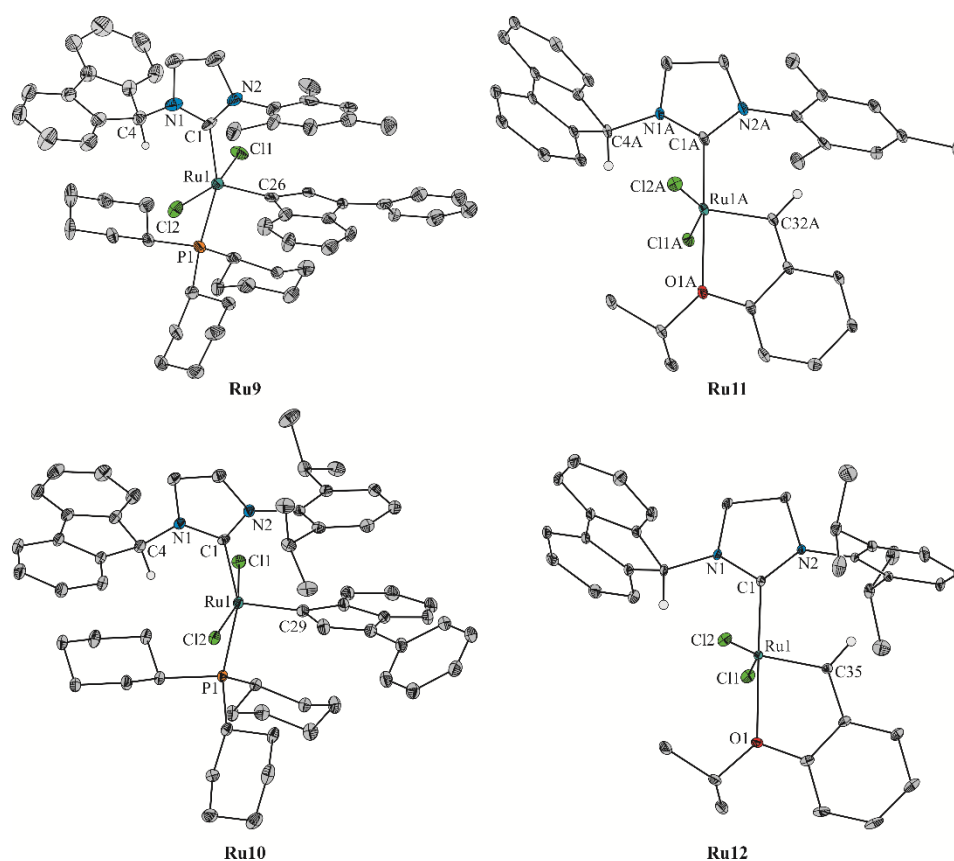


Figure 3. Molecular structures of the **Ru9–Ru12** complexes. Displacement ellipsoids are drawn at the 50% probability level. All hydrogen atoms, except those attached to the C4/C4A and C32A/C35 atoms, as well as the second independent molecule B of **Ru11** and the solvent molecules were omitted for clarity.

Table 1. Selected geometrical parameters of Ru9–Ru12.

Geometrical Parameters (Å, °)	Ru9	Ru10	Ru11 (Molecule A/Molecule B)	Ru12
Bond lengths (Å)				
C1–N1	1.324(12)	1.345(6)	1.337(8)/1.364(9)	1.349(3)
C1–N2	1.333(13)	1.343(6)	1.372(8)/1.361(8)	1.352(3)
Ru–C	2.076(9)	2.082(4)	1.974(7)/1.958(7)	1.975(2)
Ru–Cl1	2.378(2)	2.397(2)	2.325(2)/2.320(2)	2.317(2)
Ru–Cl2	2.384(2)	2.412(2)	2.331(2)/2.336(2)	2.329(2)
Ru–O	–	–	2.274(5)/2.277(5)	2.294(2)
Ru–P	2.440(2)	2.423(2)	–	–
Ru=C	1.922(11)	1.872(5)	1.850(7)/1.819(7)	1.828(2)
Angles (°)				
Cl–Ru–Cl	162.80(10)	163.55(4)	151.01(6)/149.64(6)	151.33(2)
N–C–N	110.0(8)	107.8(4)	106.5(6)/105.9(6)	106.85(18)
C–Ru–O	–	–	176.5(2)/178.8(2)	176.42(7)
C–Ru–P	156.3(3)	157.63(13)	–	–
A	81.5(5)	81.42(16)	84.49(19)/92.1(2)	97.44(8)
B	93.0(5)	100.75(19)	90.4(2)/89.3(3)	86.18(9)
C	8.5(3)	14.11(14)	–	–
D	–	–	19.8(2)/18.8(3)	11.45(10)
τ_5	0.11	0.10	0.42/0.49	0.42

Notes: A: dihedral angle between the mean-planes defined by the non-hydrogen atoms of the fluorene and the NHC moieties; B: dihedral angle between the mean-planes defined by the non-hydrogen atoms of the phenyl ring of the Mes/Dipp substituent and the NHC moiety; C: dihedral angle between the phenyl ring of the Mes/Dipp substituent and the indenylidene moiety; D: dihedral angle between the mean-planes defined by the non-hydrogen atoms of the NHC moiety and the phenyl ring of the *o*-isopropoxy-benzyl-methylene unit; τ_5 : geometry index [38].

In all four investigated complexes, the Ru(II) center is pentacoordinated (Figure 3). The indenyl derived **Ru9** and **Ru10** moieties display distorted square pyramidal coordination, while in latter Hoveyda-type complexes **Ru11** and **Ru12**, the geometry of the metallic center is intermediary between the square pyramid and trigonal bipyramid. The above statement is confirmed by the values of τ_5 , which is a structural parameter characterizing the geometry of the coordination center for five coordinated compounds [38]. In case of investigated complexes these values are 0.11, 0.10, 0.43/0.49, and 0.42 for **Ru9**, **Ru10**, **Ru11** (molecule A/molecule B), and **Ru12**, respectively. The Ru–C and Ru=C bond lengths are in the ranges from 1.958(7) up to 2.082(4) and from 1.819(7) to 1.922(11) Å, respectively, and these bonds are slightly longer in the case of both phosphine complexes. The lengths of the Ru–P bond in the **Ru9** and **Ru10** are comparable (2.440(2) and 2.423(2) Å, respectively). In turn, the Ru–O bond is slightly longer for **Ru12** (2.294(2) Å) than for **Ru11** (2.274(5)/2.277(5) Å). The distance between the Ru and O atoms within **Ru11** and **Ru12** is a bit longer than in other similar ruthenium *o*-isopropoxybenzylidene NHC complexes bearing mesityl, cyclohexyl or cyclopentyl instead of the fluorenyl [32,39–41]. The exception is an unsymmetrical Ru complex, where the NHC unit is substituted by the *N'*-diisopropylphenyl (Dipp) and cyclohexyl moieties [40]. In this case, the length of the Ru–O bond is comparable to the corresponding bond in **Ru12**.

A closer look at Figure 4 reveals that the *N*-fluorenyl group in all investigated catalysts is placed on the side opposed to alkylidene. The analysis of the angle between the mean-planes of the fluorene and the NHC ring fragments shows that for the fluorene moiety in the *o*-isopropoxy-benzylidene derivatives, the angle between the above fragments is higher than in **Ru9** and **Ru10**. In both phosphine complexes, the fluorene fragment is situated above the one of the cyclohexyl units of the PCy₃ ligand. Moreover, a specific mutual arrangement of the above-mentioned moieties in the molecule of **Ru10** results in the appearance of a weak intramolecular C–H \cdots π interaction involving the H59 atom of cyclohexane and the five-membered ring of the fluorene ($d(D\cdots A) = 3.773(6)$ Å; $\angle(D-H\cdots A) = 166^\circ$). In the above PCy₃ complexes, the presence of the mentioned substituents in a near neighborhood of

the chlorine atoms results in the increase of the Cl–Ru–Cl angle by more than 10° compared to values observed in **Ru11** and **Ru12**.

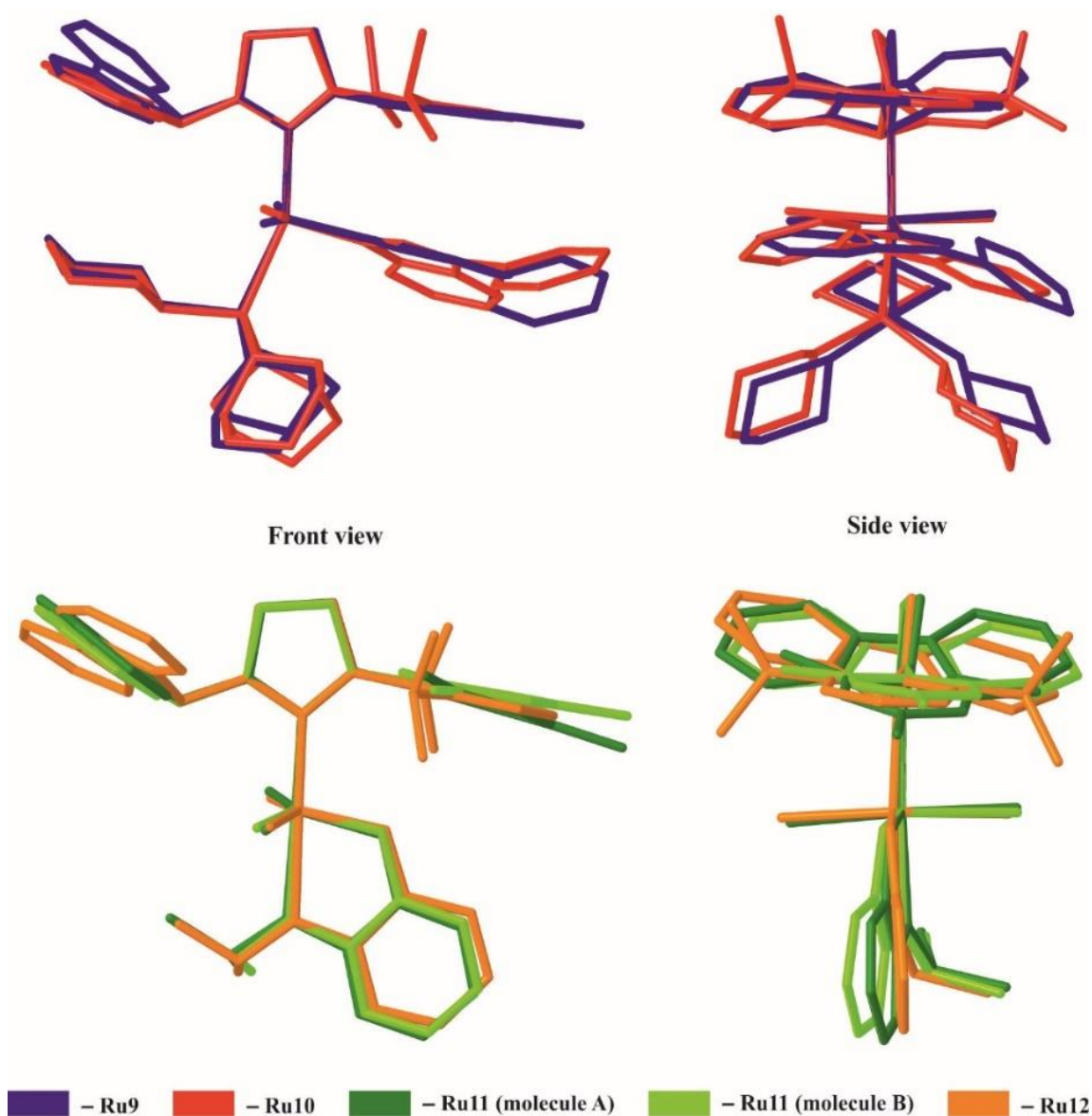


Figure 4. Superimposed molecules of **Ru9–Ru12**. The hydrogen atoms were omitted for clarity.

The aromatic rings of the mesityl and the diisopropylphenyl substituents in both phosphonium Ru complexes are positioned towards the indenylidene aromatic ring system. In the case of **Ru9**, the above moieties are inclined to each other by the angle of 8.5(3)° and the intramolecular π – π contacts were identified ($d(\text{CgI}\cdots\text{CgJ}) = 3.389(6)\text{--}3.761(6)$ Å) involving the phenyl ring of *N'*-mesityl (Mes) with the five-membered and six-membered ring of the indenylidene. In turn, in a complex bearing the more bulky diisopropylphenyl, the phenyl ring of Dipp and the indenylidene ring system are inclined towards one other by a greater degree (14.11(14)°). Here, the intramolecular π – π contact is also present, however, it involves only the phenyl ring of Dipp and the five-membered ring of indenylidene. The distance between the geometrical ring centroids of the above-mentioned rings is found to be 3.509(3) Å. It is worth mentioning that the existence of such intramolecular π – π stacking can also be observed for other Ru-PCy₃ systems containing aromatic ring fragments [13,42–46]. A comparison of the spatial orientation of the whole 3-phenyl-1*H*-inden-1-ylidene substituent shows that this moiety in **Ru9** and **Ru10** is rotated to the opposite side. In the case of **Ru11** and **Ru12**, the orientation of the

Mes and Dipp is typical for the Hoveyda-type catalysts [32,39–41,47]. Namely, the phenyl rings of the above substituents are directed towards the benzyldiene fragment in a way that the benzyldiene hydrogen is located directly under the Mes/Dipp aromatic ring. In both cases, these H-atoms and the aromatic rings adjacent to them are engaged in weak intramolecular C–H... π interactions. The distance between the donor and acceptor of the H-atom in these interactions is shortest in the case of **Ru12** (3.371(2) Å). A replacement of Mes by the bulkier Dipp substituent (see **Ru12** and **Ru11**) manifests itself in a noticeable change of the angle between the mean-planes of the NHC and phenyl ring of the benzyldiene moiety. The value of this angle is almost two times higher in the case of **Ru11** in comparison to **Ru12**.

Typically, complexes containing unsymmetrical NHC ligands display increased stability in a solution, also at elevated temperatures [22,32,48]. We were curious if fluorene moiety, combining structural elements introduced by Mauduit [32] and us [22], would also have a positive influence on catalysts' resistance towards decomposition. To explore their robustness in solvent, we prepared toluene solutions (0.02 M) of four fluorene-based catalysts and 1,3,5-trimethoxybenzene (for details see Materials and Methods section), that were heated to 50 °C and stored over 9 (for indenylidene-type complexes) and up to 40 days (for Hoveyda–Grubbs-type complexes), respectively. The degree of decomposition was determined by means of ¹H NMR (1,3,5-trimethoxybenzene was used as the internal standard). Catalysts with the *o*-isopropoxy-benzyldiene ligand, regardless of the type of uNHC, showed superior stability in comparison to their indenylidene counterparts, and the most stable complex was Dipp-bearing **Ru12** which after 10 days at 50 °C remained unchanged in 85%, and even after 40 days 70% remained intact. A little worse, but still very resilient, was its SIMes-based analogue **Ru11** (75% and 45%, respectively over the same period). Among indenylidene-type complexes, the SIMes-based uNHC **Ru9** was the least prone to decomposition (46% after 9 days), followed by its SIPr analogue **Ru10** (25% left unchanged after 9 days).

Despite some individual differences between the catalysts, one can state that the *N*-fluorenyl uNHC-based catalysts demonstrated in general improved stability in solution at elevated temperature. With this result, we opted to test their catalytic activity: first in standard model olefin metathesis reactions [49], then in some more demanding industrially-important processes, such as ethenolysis or self-metathesis of α -olefins.

First, we studied the activity profiles in ring-closing metathesis (RCM) of a relatively “easy” model substrate [49] 2,2-diallyl-tosylate (**11**) in the presence of 0.1 mol % of catalyst, in 0.1 M toluene at 50 °C (Figure 5). As expected [24], catalysts containing symmetric NHC ligands **Ru2** and **Ru5** exhibited the highest activity, reaching full conversion of **11** after only 20 and 5 min, respectively. Indenylidene based **Ru9** (Ar = Mes) and **Ru10** (Ar = Dipp) led to incomplete but high conversions but were still propagating the reaction after 90 min (no visible plateau). Interestingly, at the beginning of the reaction, complex **Ru10** initiated visibly faster than SIMes bearing **Ru2** before beginning to plateau, meaning the initially less active **Ru9** reached a similar high conversion after 90 min (Figure 5). Hoveyda–Grubbs-type complexes bearing fluorene moiety acted in a slower pace than their symmetrical NHC analogue **Ru5**, but after approximately 1 h also achieved very high conversion. Interestingly, in this case the SIMes-bearing **Ru11** acted slightly faster than its SIPr-containing analogue **Ru12** (for indenylidene-type catalysts the trend was opposite).

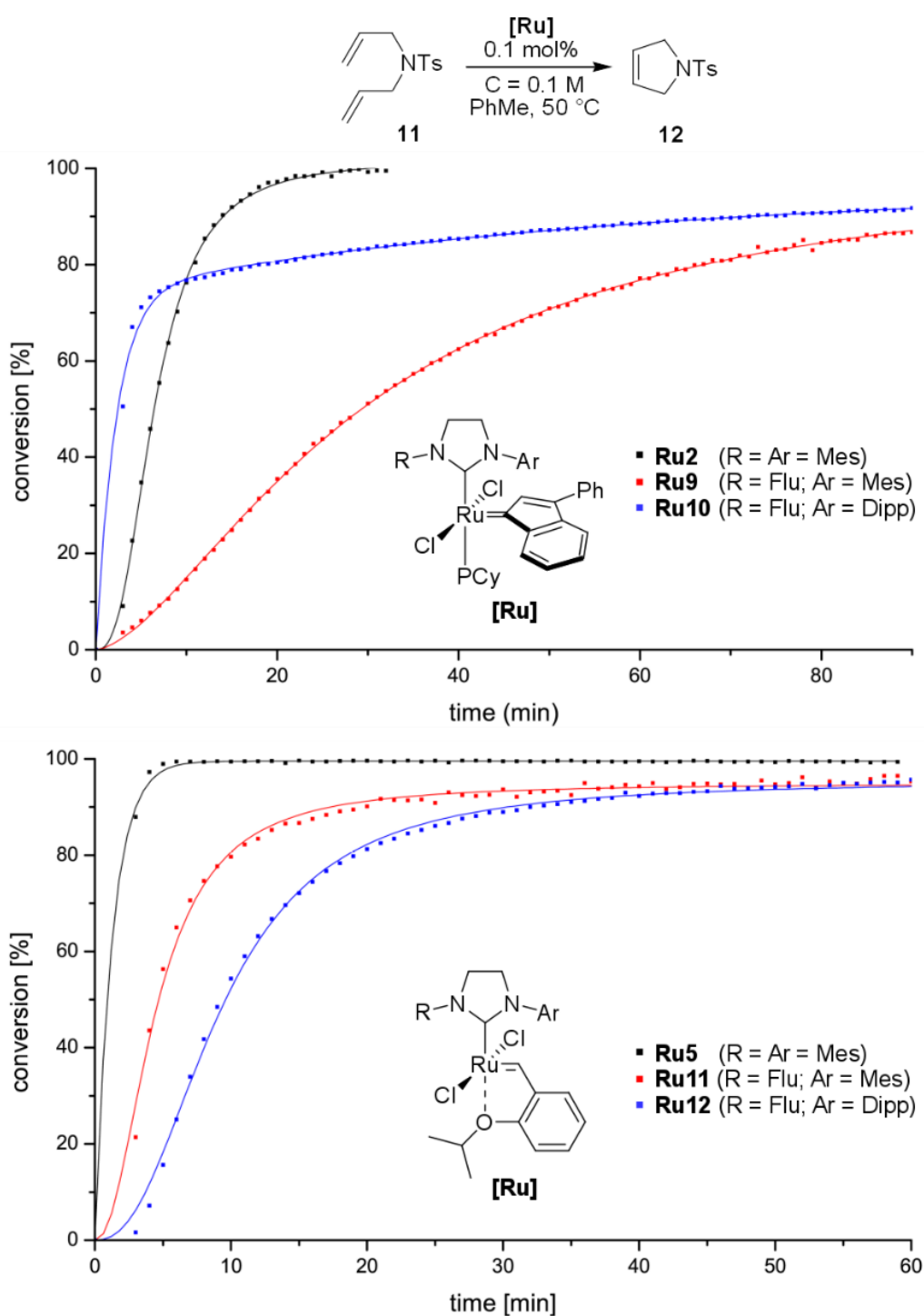


Figure 5. Time-conversion curves for ring-closing metathesis (RCM) of **11**. Flu = fluorene-9-yl. Lines are as a visual aid only.

Next, RCM of a more sterically hindered substrate, 2-allyl-2-(2-methylallyl)tosylate (**13**) [49] was performed (Figure 6) in toluene at 50 °C in the presence of 1 mol % of catalyst. In addition, general purpose complexes with symmetrical NHC ligands (**Ru2** and **Ru5**) turned out to be more efficient. Fluorene-based complexes proceeded slower, but extension of reaction time allowed complete or almost complete conversions in these cases. Similar to the RCM reaction of **11**, catalyst **Ru9** initiated a little bit faster than Umicore M2 catalyst **Ru2**, however the latter was able to outperform it quickly.

In the Hoveyda–Grubbs series the activity of catalysts with fluorene-substituted uNHC was more than satisfactory, with both leading to almost complete conversions in just over an hour.

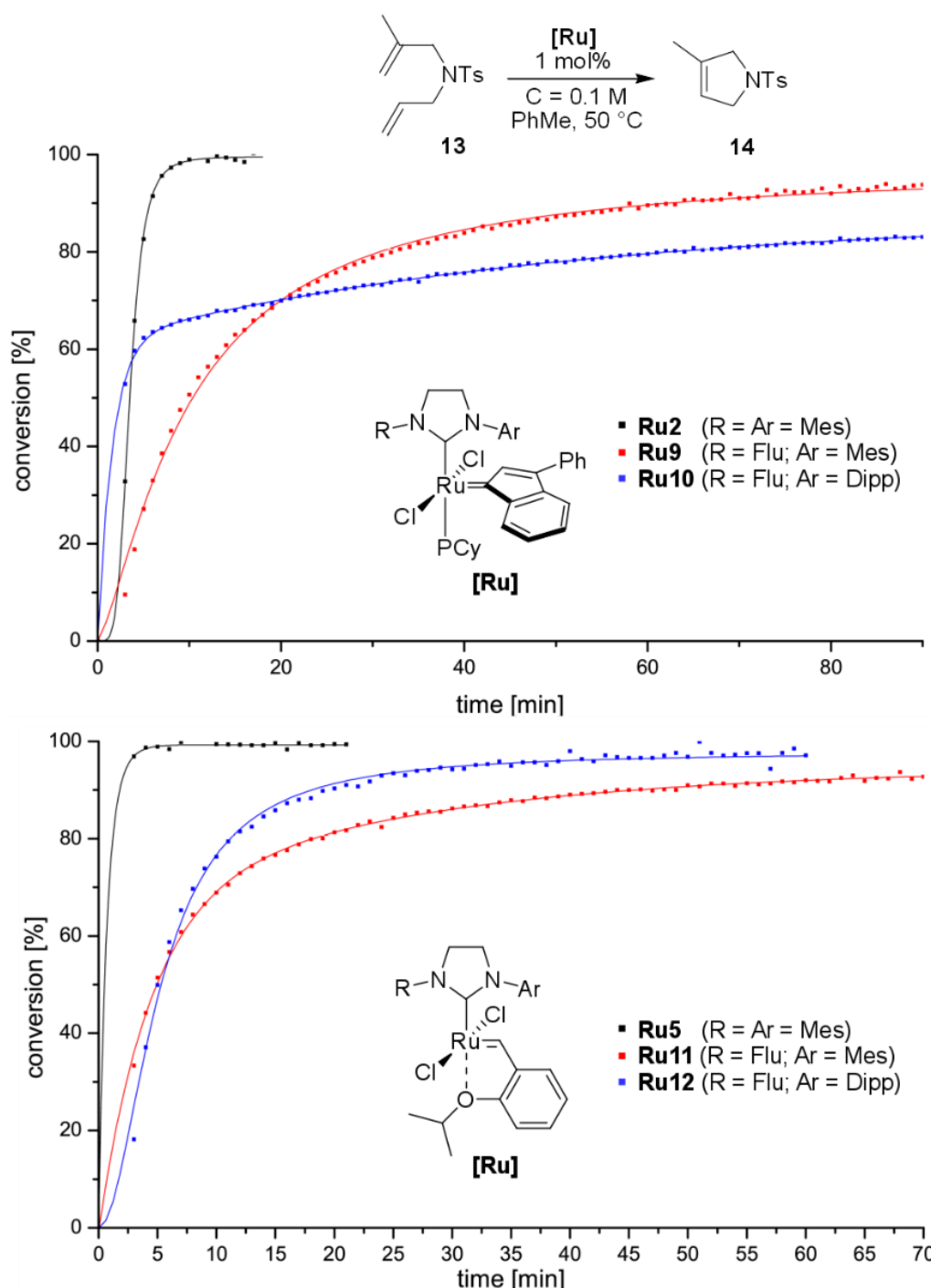
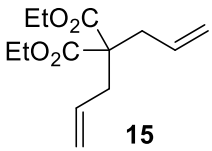
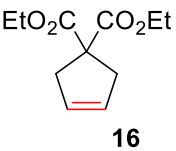
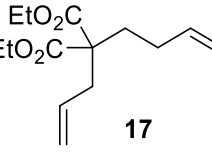
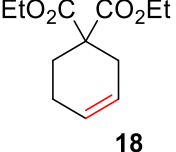
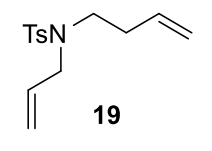
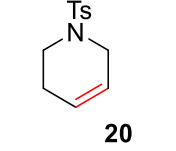
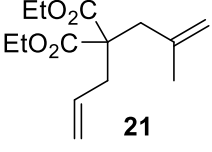
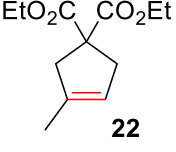
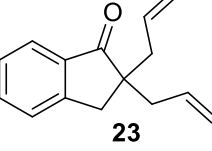
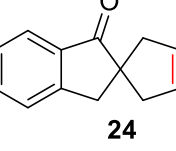
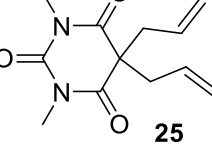
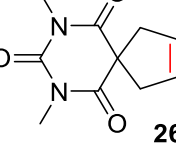


Figure 6. Time-conversion curves for RCM of **13**. Flu = fluorene-9-yl. Lines are as a visual aid only.

With the basic profiling of new uNHC complexes completed, we examined them in a more diverse set of RCM reactions (Table 2). We attempted these tests not because we believed the fluorenyl uNHC catalysts will find applications in natural products synthesis or in medicinal chemistry—the fields of applications where catalysts bearing symmetrical NHC are traditionally much more suitable [50,51]—but to be consistent with our previous studies using similar sets of more advanced substrates [26,48,52]. All reactions were performed in 0.1 M solution in toluene at 60 °C in the presence of 1000 ppm (0.1 mol %)

of catalysts to compare the new system with well-established general purpose Umicore M2 (**Ru2**) and Hoveyda–Grubbs (**Ru5**) catalysts.

Table 2. Application of fluorene-based catalysts **Ru9–Ru12** in RCM reactions.

Entry	Substrate	Product	Catalyst	Conv. (%)
1 ^a	 15	 16	Ru2	100
			Ru9	93
			Ru10	92
			Ru5	100
			Ru11	98
			Ru12	98
2	 17	 18	Ru2	100
			Ru9	99
			Ru10	96
			Ru5	100
			Ru11	87
			Ru12	96
3	 19	 20	Ru2	100
			Ru9	87
			Ru10	98
			Ru5	98
			Ru11	92
			Ru12	100
4	 21	 22	Ru2	100
			Ru9	100
			Ru10	75
			Ru5	100
			Ru11	100
			Ru12	98
5	 23	 24	Ru2	99
			Ru9	80
			Ru10	100
			Ru5	98
			Ru11	86
			Ru12	86
6	 25	 26	Ru2	100
			Ru9	67
			Ru10	84
			Ru5	100
			Ru11	62
			Ru12	98

Conditions: 0.1 mol % of catalyst, toluene (0.1 M), 60 °C, 4 h. ^a Reaction time 1.5 h.

As expected, well established catalysts **Ru2** and **Ru5** bearing symmetrical NHC gave the best results in virtually all reactions, although the newly obtained uNHC complexes also showed high activity. In the first three examples (Table 2, entries 1–3), no significant differences between these two classes of complexes were observed as the yield of the desired products was usually around 90–100%. More significant differences appeared when synthesis of a more challenging three substituted C–C double bond was attempted (entry 4), showing some advances of sterically reduced catalysts **Ru9** and **Ru11**. Substrates forming spiro-compounds were next examined. In the case of 2,2-diallyl-2,3-dihydro-1*H*-inden-1-one (**23**) (Table 2, entry 5) the drop-in conversion was not too pronounced; all catalysts achieved at least 80% conversion, with uNHC **Ru10** giving 100%. With barbituric acid derivative **25** (Table 2, entry 6), most fluorene-substituted catalysts showed limited

reactivity in comparison to general purpose symmetrical NHC complexes. Of the uNHC complexes **Ru12** gave some of the best results.

Given their high stability, complexes containing unsymmetrical NHC ligands are particularly useful in industrially relevant reactions of α -olefins—substrates particularly susceptible to migration of double bond—as well as in ethenolysis [21,24,26]. As shown before, benzyl derived indenylidene-type complex **Ru8** is more robust than standard Umicore M2 [25,31], while the *N*-cycloalkyl substituted complex **Ru7** investigated by Mauduit et al. proved to be a truly excellent catalyst for self-metathesis of α -olefin at low catalysts loading (TON, turnover number 11,680 at 50 ppm) [21]. We were curious whether the new catalysts combining structural features of the *N*-cyclopentyl and *N*-benzyl moiety into one substituent, the *N*-fluorenyl group, would outperform their parental complexes in these challenging reactions. Based on our previous results [24,35], for these tests we selected a Mes bearing, indenylidene-type complex **Ru9**, as the most optimal candidate.

Firstly, the self-metathesis reaction of 1-octene **26**, being a good representative of Fischer–Tropsch α -olefins [21], conducted neat at 80 and 50 °C with different loadings of **Ru9** was investigated. The progress of reaction was monitored by means of gas chromatography (GC). When the reaction was carried out at 80 °C in the presence of 100 ppm catalyst (Figure 7a), the fastest increase and the highest yield of the desired primary metathesis product **27** was observed, although also about 10% of unwanted byproducts, containing longer or shorter carbon chains were created (the unwanted isomerization/secondary metathesis process is a well-known and serious limitation of Ru-catalyzed self-cross metathesis (self-CM) of α -olefins) [21,53,54].

Decreasing the temperature to 50 °C (Figure 7b) slightly reduced the reaction rate—after 3 h 79% of the substrate was consumed—but at the same time significantly improved selectivity (from 87% for reaction at 80 °C, to 97% for the one performed at 50 °C). For academic research, 100 ppm of catalyst seems to be a low loading, but in industrial production it is still too high. Thus, we investigated self-CM of 1-octene at reduced catalyst loadings of 50, 10, and 1 ppm of Ru (Figure 7c–e). With decreased catalyst loadings an increase of the reaction time was necessary to achieve satisfactory substrate conversion but still maintain low levels of undesired byproducts [55]. As a result, even at 1 ppm loading of the new fluorene-containing **Ru9**, 52% conversion of **27** was reported that translates to TON of 260,000 and TOF (turn-over frequency) of 12,381 over 21 h (selectivity 89%). Self-metathesis of 1-octene was investigated at 50 ppm with other *N*-fluorenyl uNHC catalysts, and the Mes substituted Hoveyda (**Ru11**) was found to give highest selectivity (92%) but did not outperform **Ru9** (see Supplementary Materials for more details). These results indicate the superiority of the Mes substitution in *N*-fluorenyl uNHC complexes when applied to self-metathesis of 1-octene.

Finally, it shall be stressed that in the above self-CM reaction the general purpose catalysts, such as **Ru2** and **Ru5**, were reported to give very low selectivity, sometimes as low as 20% [24], probably due to extensive catalysts decomposition forming Ru-hydride species [56,57], dimers [29], and possibly other yet undefined species.

Ethenolysis is another industrially relevant process enabling valorization of biomass [58–60]. This process is usually carried out in the presence of specialized cyclic alkyl amino carbene (CAAC)- or uNHC-bearing complexes, as the general-purpose SIMes and SIPr Ru catalysts give suboptimal results in this case [16,18,19,61–64].

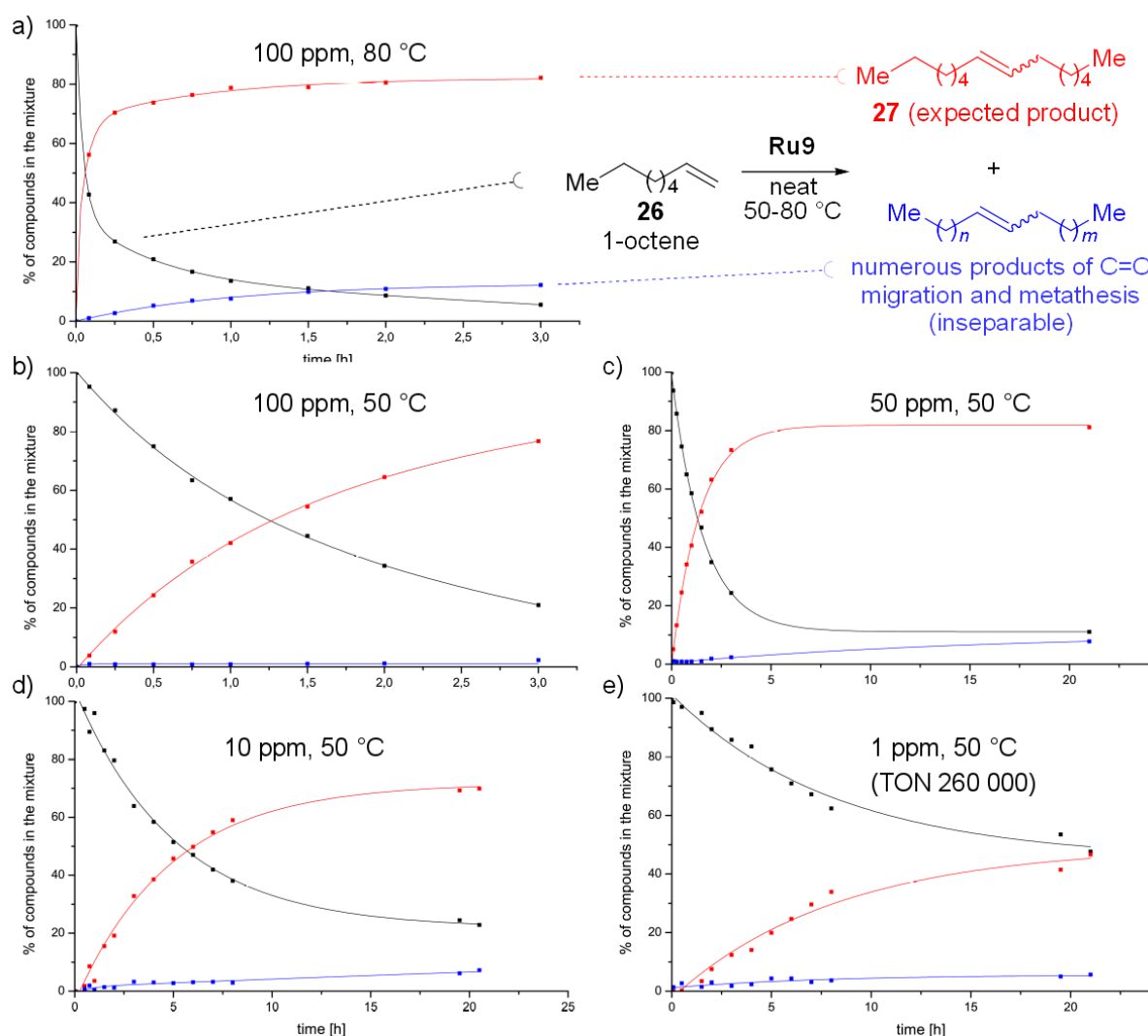


Figure 7. Self-cross metathesis (self-CM) of 1-octene. (a) Ru9 100 ppm, 80 °C. (b) Ru9 100 ppm, 50 °C. (c) Ru9 50 ppm, 50 °C. (d) Ru9 10 ppm, 50 °C. (e) Ru9 1 ppm, 50 °C. Lines are as a visual aid only.

Therefore, we opted to check how the new uNHC complexes work in this case. To do so, we selected ethyl oleate as a model substrate (oleic acid esters are commonly used for such purpose) under industrially-friendly conditions [19,48] (i.e., in an ordinary steel autoclave outside a glovebox using ethylene grade 3). Some preliminary studies have shown that the lowest Ru loading where our catalysts are still giving practically useful conversions is equivalent to 100 ppm. Under such conditions, the bulkier Dipp-bearing fluorenyl catalysts (**Ru10**, **Ru12**) gave good results, both in terms of conversion and selectivity (Figure 8). Interestingly, the Mes-derived fluorenyl catalysts (**Ru9**, **Ru11**) performed with lower conversion, however, exhibiting only slightly reduced selectivity. These results (TON up to 7140) obtained for **Ru10** and **Ru12** outperform not only earlier Ru uNHC complexes [16] but also more recent complexes bearing uNHC with a thiophene wing, as well the recently disclosed Ru complex bearing highly engineered bulky phenanthrene-based uNHC, which under the same conditions provided TON of 4550 [19] and 1370, respectively [48]. It shall be at the same time noted, however, that our fluorenyl uNHC catalysts that need 100 ppm to maintain acceptable conversion are less powerful than CAAC complexes, such as **Ru13**, which was reported to work in ethenolysis with grade 3 ethylene under similar conditions at 25 ppm resulting in TONs up to 28,000 [63].

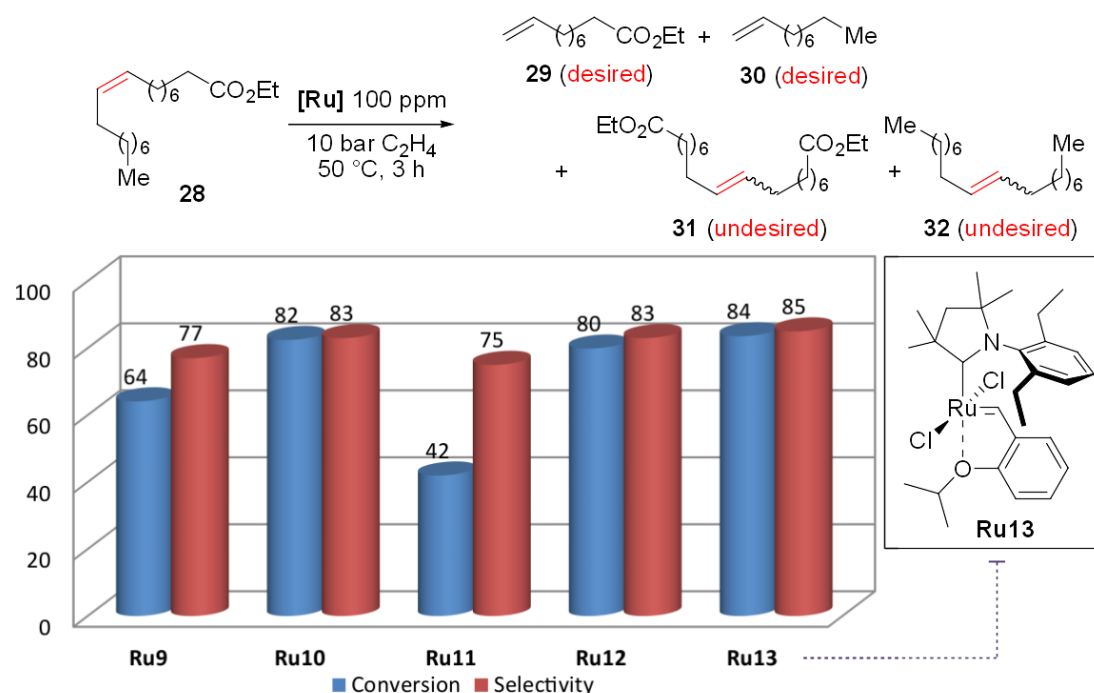


Figure 8. Ethenolysis of ethyl oleate (**28**) with ethylene grade 3. Conversion and selectivity were calculated from gas chromatography (GC). Conversion = $100 - ((\text{final moles of } \mathbf{28}) \times 100 / (\text{initial moles of } \mathbf{28}))$; Selectivity = $100 \times (\text{moles of } \mathbf{29} + \mathbf{30}) / ((\text{moles of } \mathbf{29} + \mathbf{30}) + (2 \times \text{moles of } \mathbf{31} + \mathbf{32}))$.

3. Materials and Methods

3.1. General

All reagents were purchased from Sigma-Aldrich, Apeiron, Strem, TCI, and Alfa Aesar and used without further purification unless stated otherwise. Reactions which required use of moisture and oxygen-free conditions were performed using the Schlenk technique or in a glovebox, under an atmosphere of argon with use of dry and degassed solvents from SPS (Solvent Purification System). The stock solutions of catalyst were prepared in the glovebox under moisture and oxygen-free conditions. Analytical thin-layer chromatography (TLC) was performed using silica gel 60 F254 precoated plates (0.25 mm thickness) with a fluorescent indicator. Visualization of TLC plates was performed by UV light or by KMnO_4 water solution. Flash chromatography was performed using silica gel 60 (230–400 mesh). GC analysis was done using Clarus 580 chromatograph using tetradecane as an internal standard. ^1H and ^{13}C NMR spectra were recorded on an Agilent 400-MR DD2 400 MHz spectrometer. Chemical shifts (δ) are given in ppm with coupling constants (J) in Hz; they are reported relative to reference solvent peaks in deuterated solvent: 7.26 and 77.16 ppm for ^1H and ^{13}C NMR, respectively in CDCl_3 ; 5.32 and 53.84 ppm for ^1H and ^{13}C NMR, respectively in CD_2Cl_2 . The following abbreviations are used to denote multiplicity: s-singlet, d-doublet, t-triplet, q-quartet, m-multiplet, dd-doublet of doublets, dt-doublet of triplets, ddd-doublet of doublets of doublets. IR spectra were recorded on JASCO FT/IR-6200 spectrometer. Wavenumbers are given in cm^{-1} . High resolution electrospray mass spectroscopy (ESI-HRMS) was obtained on AutoSpec Premier spectrometer. Melting points were recorded on an OptiMelt SRS apparatus with a heating rate of $10^\circ\text{C}/\text{min}$.

3.2. Synthesis of New Complexes

Synthesis of complex Ru10. The pentafluorobenzene adduct (338 mg, 0.600 mmol, 1.1 equiv.) was weighed into an oven-dried Schlenk flask under argon and dissolved in dry toluene (3 mL). Umicore M1 (504 mg, 0.545 mmol, 1.0 equiv.) was added and the resulting red/brown reaction mixture was stirred at 90°C (in preheat oil bath). The reaction mixture was monitored by TLC over a period of 5 h as

significant amounts of start material appeared to be present. Phosphine scavenger copper (I) chloride (27 mg, 0.273 mmol, 0.5 equiv.) was added and the mixture was reacted for another hour. After cooling, the reaction mixture was diluted with *n*-hexane (10 mL) and placed onto a short column packed in neat hexane. The column was eluted with neat hexane to remove toluene before eluting with 1% ethyl acetate/*n*-hexane until all start material was removed, then the polarity was gradually increased to 5% (in 1% increments) to elute the product. After evaporation the product was recrystallized from *n*-hexane affording the product as a red crystalline solid (200 mg, 193 μ mol, 35%). ^1H NMR (400 MHz, CD_2Cl_2) δ 8.77 (dd, $J = 7.4, 1.3$ Hz, 1H), 8.69–8.55 (m, 1H), 8.34 (dd, $J = 7.4, 1.0$ Hz, 1H), 7.83–7.75 (m, 2H), 7.65–7.57 (m, 3H), 7.56–7.35 (m, 7H), 7.29–7.15 (m, 2H), 7.14–7.04 (m, 1H), 6.90 (s, 1H), 6.85 (t, $J = 7.7$ Hz, 1H), 6.59 (ddd, $J = 26.4, 7.8, 1.5$ Hz, 2H), 4.09–3.87 (m, 1H), 3.83–3.66 (m, 1H), 3.55–3.40 (m, 1H), 3.36–3.17 (m, 2H), 3.02 (hept, $J = 6.6$ Hz, 1H), 2.45–2.19 (m, 3H), 1.76 (d, $J = 13.9$ Hz, 6H), 1.55–1.35 (m, 5H), 1.28 (dt, $J = 12.3, 3.1$ Hz, 8H), 1.21 (d, $J = 6.6$ Hz, 3H), 1.03 (d, $J = 6.9$ Hz, 3H), 0.85 (d, $J = 6.8$ Hz, 3H), 0.74 (d, $J = 6.6$ Hz, 3H). ^{13}C NMR (101 MHz, CD_2Cl_2) δ 216.9 (d, $J = 71.2$ Hz), 147.7, 147.1, 144.6, 142.1, 141.8, 141.7, 141.7, 141.6, 139.0, 137.5, 137.4, 137.2, 130.7, 129.8, 129.1, 128.9, 128.3, 128.2, 128.1, 128.1, 127.9, 127.3, 124.3, 123.8, 120.3, 116.9, 65.0, 55.6, 44.0, 43.9, 32.9, 32.7, 30.2, 29.7, 28.5, 28.3, 28.2, 28.2, 28.1, 28.1, 27.5, 27.4, 27.1, 26.7, 26.0, 23.3, 22.5. ^{31}P NMR (162 MHz, CD_2Cl_2) δ 31.62. IR (neat): ν 3052, 2926, 2849, 1588, 1537, 1476, 1436, 1838, 1358, 1338, 1322, 1295, 1257, 1200, 1173, 1130, 1107, 1048, 1027, 1005, 977, 949, 916, 886, 848, 819, 801, 774, 747, 697, 681, 647, 621, 583, 555, 505, 490, 420 cm^{-1} . HRMS (ESI): m/z calculated for $\text{C}_{61}\text{H}_{73}\text{Cl}_2\text{N}_2\text{PRu} [\text{M}]^+$ 1036.3932, found 1036.3932.

Synthesis of complex **Ru11**. Hoveyda–Grubbs I (210 mg, 0.35 mmol, 1 equiv.) and the corresponding pentafluorobenzene adduct (200 mg, 0.385 mmol, 1.1 equiv.) were weighed into an oven-dried Schlenk tube under argon and sealed with a septum. Toluene (3 mL) was added and the reaction mixture was heated to 90 °C (in preheated oil bath) for 30 min, monitoring progress by TLC. Copper (I) chloride (38.5 mg, 0.385 mmol, 1.1 equiv.) was added, and the reaction mixture was heated for a further 10 min. The cooled reaction mixture was poured onto a column of silica packed in neat hexane and flushed with neat hexane until the toluene was removed. The column was then eluted with a silica's length of 5% and then 10% ethyl acetate/*n*-hexane collecting a red/brown fraction; the product was then eluted with 20% ethyl acetate/*n*-hexane. Fractions containing product were concentrated in vacuo; the crude product was redissolved in DCM and MeOH and concentrated at the rotary evaporator without heating. After evaporation of DCM, the methanol and other liquids were removed with a syringe from the green crystals. The process was once again repeated. The product crystallized as lustrous dark green crystals (175 mg, 0.26 mmol, 74%). ^1H NMR (400 MHz, CD_2Cl_2) δ 16.25 (s, 1H), 8.37 (d, $J = 7.5$ Hz, 2H), 7.81 (dd, $J = 7.5, 1.0$ Hz, 2H), 7.59 (dddd, $J = 8.5, 5.2, 3.8, 0.9$ Hz, 1H), 7.49 (td, $J = 7.5, 0.9$ Hz, 2H), 7.41 (tt, $J = 7.6, 1.1$ Hz, 2H), 7.29 (s, 1H), 7.13 (s, 2H), 7.01 (d, $J = 0.9$ Hz, 2H), 7.00–6.98 (m, 1H), 5.14 (dq, $J = 12.4, 6.2$ Hz, 1H), 3.89–3.78 (m, 2H), 3.32–3.22 (m, 2H), 2.49 (s, 3H), 2.29 (s, 6H), 1.62 (dd, $J = 6.2, 0.9$ Hz, 6H), 1.53 (d, $J = 0.9$ Hz, 2H). ^{13}C NMR (101 MHz, CD_2Cl_2) δ 209.1, 152.8, 144.6, 142.4, 141.6, 139.6, 138.6, 138.5, 130.1, 129.7, 128.3, 127.7, 123.1, 122.9, 120.4, 113.5, 76.0, 75.9, 65.3, 65.3, 43.9, 22.3, 21.5, 18.4, 18.4. IR (neat): $\nu = 2975, 1473, 1436, 1411, 1327, 1260, 1217, 1156, 1109, 1096, 933, 842, 747, 680$ cm^{-1} . HRMS (ESI): m/z calculated for $\text{C}_{35}\text{H}_{36}\text{Cl}_2\text{N}_2\text{ORuNa} [\text{M} + \text{Na}]^+$ 695.1146, found 695.1123.

Synthesis of complex **Ru12**. Hoveyda–Grubbs I catalyst (485 mg, 0.81 mmol, 1 equiv.) and the corresponding pentafluorobenzene adduct (500 mg, 0.89 mmol, 1.1 equiv.) were added to a Schlenk flask and argonated. Dry toluene (6 mL) was added and the resulting dark brown mixture was stirred for about 30 min at 80 °C. The reaction was monitored by TLC. When the reaction was complete, phosphine scavenger copper (I) chloride (121 mg, 1.21 mmol, 1.5 equiv.) was added and the mixture was stirred for a further 10 min and checked by TLC. After cooling the mixture was put onto a column packed in neat hexane and then eluted with *n*-hexane to remove the toluene. The column was eluted with the silica's length of 5% ethyl acetate/*n*-hexane followed by 10% ethyl acetate/*n*-hexane until the red/brown fraction was collected. The product was then eluted with 20% ethyl acetate/*n*-hexane. Product fractions were checked by TLC, collected into one flask, concentrated to dryness, and recrystallized from DCM/MeOH on the rotary evaporator. The product was obtained

as lustrous dark green crystals (389 mg, 0.54 mmol, 67%). ^1H NMR (400 MHz, CD_2Cl_2) δ 16.23 (d, $J = 0.9$ Hz, 1H), 8.41–8.37 (m, 2H), 7.82 (ddd, $J = 7.5, 1.2, 0.7$ Hz, 2H), 7.69–7.61 (m, 1H), 7.56 (ddd, $J = 8.3, 6.1, 3.0$ Hz, 1H), 7.50 (tdd, $J = 7.5, 1.2, 0.6$ Hz, 2H), 7.47–7.39 (m, 4H), 7.34 (s, 1H), 7.00 (dt, $J = 8.3, 0.7$ Hz, 1H), 6.96–6.92 (m, 2H), 5.19–5.08 (m, 1H), 3.94–3.72 (m, 2H), 3.35–3.15 (m, 4H), 1.65 (d, $J = 6.1$ Hz, 6H), 1.22 (d, $J = 7.0$ Hz, 6H), 0.95 (d, $J = 6.7$ Hz, 6H). ^{13}C NMR (101 MHz, CD_2Cl_2) δ 149.0, 142.4, 141.6, 130.2, 130.0, 129.7, 128.3, 127.7, 125.4, 123.0, 122.6, 120.3, 113.5, 76.0, 65.5, 55.6, 43.6, 28.6, 25.9, 24.2, 22.5. IR (neat): ν 3063, 3049, 2923, 2892, 2866, 1958, 1918, 1823, 1720, 1604, 1588, 1575, 1477, 1449, 1429, 1419, 1384, 1337, 1316, 1294, 1266, 1249, 1217, 1177, 1158, 1142, 1111, 1098, 1049, 1037, 1021, 1003, 981, 951, 932, 879, 842, 810, 794, 756, 745, 680, 657, 640, 620, 582, 492, 438, 418 cm^{-1} . HRMS (ESI): m/z calculated for $\text{C}_{38}\text{H}_{42}\text{Cl}_2\text{N}_2\text{ORuNa}$ [$M + \text{Na}$] $^+$ 737.1615, found 695.1608.

3.3. Catalysis

General procedure for thermal stability studies. In a Young NMR tube, the corresponding catalyst (12.8 μmol) was dissolved in 0.65 mL of toluene- d_8 followed by addition of 0.13 M solution of 1,3,5-trimethoxybenzene in toluene- d_8 (internal standard, 50 μL , 6.4 μmol) in a glove box. An NMR tube was removed from the glove box and placed in a preheated (50 $^\circ\text{C}$) water bath. ^1H NMR spectra were recorded in frequent time intervals. Degradation of catalyst was calculated by comparing the integration of benzylidene and indenylidene signal in complexes and 9 protons from methoxy groups in internal standard.

General procedure for model RCM reactions. The substrate was accurately weighed into a Radley carousel under inert atmosphere and dissolved in dry toluene (3.8 mL) with stirring. In the glovebox the catalyst (0.01 mmol) was dissolved in dry toluene (2 mL), then 0.2 mL of this stock solution were transferred to the reaction mixture and heated at 80 $^\circ\text{C}$ overnight under a flow of argon. The reaction was cooled, quenched with SnatchCat and concentrated in vacuo before being dispersed on 70–230 Silica and purifying on the Combi-flash. Concentration of fractions afforded the pure products. ^1H NMR analysis was done to determine the structure of each product.

General procedure for α -olefin metathesis. In the glovebox a stock solution of catalyst was made up in a 1 mL volumetric flask. A solution of 1-octene (1.5 mL, 9.37 mmol) in tetradecane (0.5 mL, 1.9 mmol) as internal standard was stirred at a certain temperature before a sample without catalyst was taken. The appropriate volume of stock solution was added via micro syringe to the reaction mixture before reaction samples (0.1 mL) for GC analysis were taken at relevant time intervals. Samples were quenched with SnatchCat solution (35 μmol , 1 mL). Conversion and selectivity were determined by GC measurement according to the calculations below.

General procedure for ethenolysis reaction. Into a dry autoclave tube charged with ethyl oleate (**28**) (purified by passing through an Al_2O_3 pad, 4.66 g, 15 mmol) and tetradecane (internal standard, 0.61 g, 3 mmol), the stock solution of catalyst (100 ppm, dissolved in 0.1 mL of HPLC grade DCM) was added. The autoclave was closed, purged with ethylene (3 times), and stirred at 50 $^\circ\text{C}$ for 3 h with 10 bar continuous ethylene pressure. On completion the reaction was quenched by ethyl-vinyl ether addition. Conversion and selectivity were determined by GC measurement.

4. Conclusions

New indenylidene- and Hoveyda–Grubbs-type complexes with fluorene-based NHC ligands were obtained via direct reaction between pentafluorophenyl-adducts **9** and **10** and corresponding Ru complexes **Ru1** and **Ru4**. The introduction of fluorene moiety in conjunction with either the Mes or Dipp group was found to have a profound influence on stability and activity of the resulting catalysts, especially in reactions of demanding substrates, such as cross-metathesis of oleic substrate with ethylene and self-CM of α -olefins. For ethenolysis, the Dipp substituted *N*-fluorenyl uNHC complexes (independent of their initiating alkylidene) gave results better than some other recently disclosed uNHC systems [48], but worse than modern engineered CAAC and bis(CAAC) systems [62,63]. Importantly, in the self-CM of α -olefins, the Mes substituted *N*-fluorenyl uNHC complexes performed very well,

making it possible to decrease catalysts loading of **Ru9** to 1 ppm and obtain the desired primary metathesis product **27** with high efficiency (TON = 260,000) and selectivity. Therefore, despite catalysts **Ru9–Ru12** not being universal as the general-purpose Umicore M2 or Hoveyda–Grubbs systems (**Ru2**, **Ru5**), we believe that their superior performance in self-metathesis can find a number of important applications, especially in the industrial context.

Supplementary Materials: The following are available online at <http://www.mdpi.com/2073-4344/10/6/599/s1> Data concerning crystallography data for this paper (CCDC 1979853–1979856) can be obtained freely via http://www.ccdc.cam.ac.uk/data_request/cif, by e-mailing data_request@ccdc.cam.ac.uk, or by contacting directly the Cambridge Crystallographic Data Centre (12 Union Road, Cambridge CB2 1EZ, UK. Fax: +44 1223 336033).

Author Contributions: Conceptualization, K.G.; investigation, P.I.J., A.M., P.M. and D.T.; writing—original draft preparation, A.K. and K.G.; writing—review and editing, D.T., K.W., A.K. and K.G.; visualization, K.G., P.M. and A.K.; supervision, P.I.J., K.W., A.K. and K.G.; funding acquisition, P.I.J. All authors have read and agreed to the published version of the manuscript.

Funding: P.I.J. is grateful to the POLONEZ project financed from the National Science Centre, Poland on the basis of decision DEC-2016/21/P/ST5/04016. This project received funding from the European Union’s Horizon 2020 research and innovation programme under the Marie Skłodowska-Curie grant agreement No. 665778. The study was carried out at the Biological and Chemical Research Centre, University of Warsaw, established within the project co-financed by the European Union from the European Regional Development Fund under the Operational Programme Innovative Economy, 2007–2013. The X-ray diffraction data collection was collected at the Core Facility for crystallographic and biophysical research to support the development of medicinal products established within the TEAM-TECH Core Facility programme of the Foundation for Polish Science co-financed by the European Union under the European Regional Development Fund.

Conflicts of Interest: The authors declare no conflicts of interest.

References and Notes

1. Grela, K. *Olefin Metathesis: Theory and Practice*; John Wiley & Sons, Inc.: Hoboken, NJ, USA, 2014.
2. Grubbs, R.H.; Wenzel, A.G.; O’Leary, D.J.; Khosravi, E. *Handbook of Metathesis*; Wiley-VCH: Weinheim, Germany, 2015.
3. 12 Principles of Green Chemistry. Available online: <https://www.acs.org/content/acs/en/greenchemistry/principles/12-principles-of-green-chemistry.html> (accessed on 4 May 2020).
4. Nguyen, S.T.; Johnson, L.K.; Grubbs, R.H.; Ziller, J.W. Ring-opening metathesis polymerization (ROMP) of norbornene by a group viii carbene complex in protic media. *J. Am. Chem. Soc.* **1992**, *114*, 3974–3975. [[CrossRef](#)]
5. Piola, L.; Nahra, F.; Nolan, S.P. Olefin metathesis in air. *Beilstein J. Org. Chem.* **2015**, *11*, 2038–2056. [[CrossRef](#)] [[PubMed](#)]
6. Huang, J.; Stevens, E.D.; Nolan, S.P.; Petersen, J.L. Olefin metathesis-active ruthenium complexes bearing a nucleophilic carbene ligand. *J. Am. Chem. Soc.* **1999**, *121*, 2674–2678. [[CrossRef](#)]
7. Scholl, M.; Trnka, T.M.; Morgan, J.P.; Grubbs, R.H. Increased ring closing metathesis activity of ruthenium-based olefin metathesis catalysts coordinated with imidazolin-2-ylidene ligands. *Tetrahedron Lett.* **1999**, *40*, 2247–2250. [[CrossRef](#)]
8. Ackermann, L.; Fürstner, A.; Weskamp, T.; Kohl, F.J.; Herrmann, W.A. Ruthenium carbene complexes with imidazolin-2-ylidene ligands allow the formation of tetrasubstituted cycloalkenes by RCM. *Tetrahedron Lett.* **1999**, *40*, 4787–4790. [[CrossRef](#)]
9. Paradiso, V.; Costabile, C.; Grisi, F. Ruthenium-based olefin metathesis catalysts with monodentate unsymmetrical NHC ligands. *Beilstein J. Org. Chem.* **2018**, *14*, 3122–3149. [[CrossRef](#)]
10. Hamad, F.B.; Sun, T.; Xiao, S.; Verpoort, F. Olefin metathesis ruthenium catalysts bearing unsymmetrical heterocyclic carbenes. *Coord. Chem. Rev.* **2013**, *257*, 2274–2292. [[CrossRef](#)]
11. Fürstner, A.; Ackermann, L.; Gabor, B.; Goddard, R.; Lehmann, C.W.; Mynott, R.; Stelzer, F.; Thiel, O.R. Comparative investigation of ruthenium-based metathesis catalysts bearing *N*-heterocyclic carbene (NHC) ligands. *Chemistry* **2001**, *7*, 3236–3253. [[CrossRef](#)]
12. Vehlou, K.; Gessler, S.; Blechert, S. Deactivation of ruthenium olefin metathesis catalysts through intramolecular carbene–arene bond formation. *Angew. Chem. Int. Ed.* **2007**, *46*, 8082–8085. [[CrossRef](#)]

13. Ledoux, N.; Allaert, B.; Pattyn, S.; Mierde, H.V.; Vercaemst, C.; Verpoort, F. *N,N'*-dialkyl- and *N*-alkyl-*N*-mesityl-substituted *n*-heterocyclic carbenes as ligands in grubbs catalysts. *Chemistry* **2006**, *12*, 4654–4661. [[CrossRef](#)]
14. Samojłowicz, C.; Bieniek, M.; Grela, K. Ruthenium-based olefin metathesis catalysts bearing *N*-heterocyclic carbene ligands. *Chem. Rev.* **2009**, *109*, 3708–3742. [[CrossRef](#)] [[PubMed](#)]
15. Vougioukalakis, G.C.; Grubbs, R.H. Ruthenium-based heterocyclic carbene-coordinated olefin metathesis catalysts. *Chem. Rev.* **2009**, *110*, 1746–1787. [[CrossRef](#)]
16. Thomas, R.M.; Keitz, B.K.; Champagne, T.M.; Grubbs, R.H. Highly selective ruthenium metathesis catalysts for ethenolysis. *J. Am. Chem. Soc.* **2011**, *133*, 7490–7496. [[CrossRef](#)] [[PubMed](#)]
17. Engl, P.S.; Fedorov, A.; Copéret, C.; Togni, A. *N*-trifluoromethyl NHC ligands provide selective ruthenium metathesis catalysts. *Organometallics* **2016**, *35*, 887–893. [[CrossRef](#)]
18. Paradiso, V.; Bertolasi, V.; Costabile, C.; Caruso, T.; Dąbrowski, M.; Grela, K.; Grisi, F. Expanding the family of Hoveyda–Grubbs catalysts containing unsymmetrical NHC ligands. *Organometallics* **2017**, *36*, 3692–3708. [[CrossRef](#)]
19. Wyrębek, P.; Małecki, P.; Sytniczuk, A.; Kośnik, W.; Gawin, A.; Kostrzewa, J.; Kajetanowicz, A.; Grela, K. Looking for the noncyclic(amino)(alkyl)carbene ruthenium catalyst for ethenolysis of ethyl oleate: Selectivity is on target. *ACS Omega* **2018**, *3*, 18481–18488. [[CrossRef](#)]
20. Thomas, R.M.; Fedorov, A.; Keitz, B.K.; Grubbs, R.H. Thermally stable, latent olefin metathesis catalysts. *Organometallics* **2011**, *30*, 6713–6717. [[CrossRef](#)]
21. Rouen, M.; Queval, P.; Borré, E.; Falivene, L.; Poater, A.; Berthod, M.; Hugues, F.; Cavallo, L.; Baslé, O.; Olivier-Bourbigou, H.; et al. Selective metathesis of α -olefins from bio-sourced Fischer–Tropsch feeds. *ACS Catal.* **2016**, *6*, 7970–7976. [[CrossRef](#)]
22. Małecki, P.; Gajda, K.; Ablialimov, O.; Malińska, M.; Gajda, R.; Woźniak, K.; Kajetanowicz, A.; Grela, K. Hoveyda–Grubbs-type precatalysts with unsymmetrical *n*-heterocyclic carbenes as effective catalysts in olefin metathesis. *Organometallics* **2017**, *36*, 2153–2166. [[CrossRef](#)]
23. Kavitate, S.; Samantaray, M.K.; Dehn, R.; Deuerlein, S.; Limbach, M.; Schachner, J.A.; Jeanneau, E.; Coperet, C.; Thieuleux, C. Unsymmetrical Ru–NHC catalysts: A key for the selective tandem ring opening–ring closing alkene metathesis (RO–RCM) of cyclooctene. *Dalton Trans.* **2011**, *40*, 12443–12446. [[CrossRef](#)]
24. Małecki, P.; Gajda, K.; Gajda, R.; Woźniak, K.; Trzaskowski, B.; Kajetanowicz, A.; Grela, K. Specialized ruthenium olefin metathesis catalysts bearing bulky unsymmetrical nhc ligands: Computations, synthesis, and application. *ACS Catal.* **2019**, *9*, 587–598. [[CrossRef](#)]
25. Ablialimov, O.; Kędziołek, M.; Malińska, M.; Woźniak, K.; Grela, K. Synthesis, structure, and catalytic activity of new ruthenium(II) indenylidene complexes bearing unsymmetrical *N*-heterocyclic carbenes. *Organometallics* **2014**, *33*, 2160–2171. [[CrossRef](#)]
26. Smoleń, M.; Kośnik, W.; Gajda, R.; Woźniak, K.; Skoczeń, A.; Kajetanowicz, A.; Grela, K. Ruthenium complexes bearing thiophene-based unsymmetrical *N*-heterocyclic carbene ligands as selective catalysts for olefin metathesis in toluene and environmentally friendly 2-methyltetrahydrofuran. *Chemistry* **2018**, *24*, 15372–15379. [[CrossRef](#)] [[PubMed](#)]
27. Sytniczuk, A.; Dąbrowski, M.; Banach, Ł.; Urban, M.; Czarnocka-Śniadała, S.; Milewski, M.; Kajetanowicz, A.; Grela, K. At long last: Olefin metathesis macrocyclization at high concentration. *J. Am. Chem. Soc.* **2018**, *140*, 8895–8901. [[CrossRef](#)] [[PubMed](#)]
28. Hong, S.H.; Wenzel, A.G.; Salguero, T.T.; Day, M.W.; Grubbs, R.H. Decomposition of ruthenium olefin metathesis catalysts. *J. Am. Chem. Soc.* **2007**, *129*, 7961–7968. [[CrossRef](#)]
29. Higman, C.S.; Plais, L.; Fogg, D.E. Isomerization during olefin metathesis: An assessment of potential catalyst culprits. *ChemCatChem* **2013**, *5*, 3548–3551. [[CrossRef](#)]
30. Higman, C.S.; Lanterna, A.E.; Marin, M.L.; Scaiano, J.C.; Fogg, D.E. Catalyst decomposition during olefin metathesis yields isomerization-active ruthenium nanoparticles. *ChemCatChem* **2016**, *8*, 2446–2449. [[CrossRef](#)]
31. Ablialimov, O.; Kędziołek, M.; Torborg, C.; Malińska, M.; Woźniak, K.; Grela, K. New ruthenium(II) indenylidene complexes bearing unsymmetrical *N*-heterocyclic carbenes. *Organometallics* **2012**, *31*, 7316–7319. [[CrossRef](#)]
32. Rouen, M.; Borre, E.; Falivene, L.; Toupet, L.; Berthod, M.; Cavallo, L.; Olivier-Bourbigou, H.; Mauduit, M. Cycloalkyl-based unsymmetrical unsaturated (U2)-NHC ligands: Flexibility and dissymmetry in ruthenium-catalysed olefin metathesis. *Dalton Trans.* **2014**, *43*, 7044–7049. [[CrossRef](#)]

33. For an alternative approach where a sterically reduced NHC ligand, bearing a CF₃ wing gave a very selective Ru catalyst, see ref [17].
34. Benhamou, L.; Bastin, S.; Lugan, N.; Lavigne, G.; César, V. Metal-assisted conversion of an *N*-ylide mesomeric betaine into its carbenic tautomer: Generation of *N*-(fluoren-9-yl)imidazol-2-ylidene complexes. *Dalton Trans.* **2014**, *43*, 4474–4482. [[CrossRef](#)]
35. Jolly, P.I.; Marczyk, A.; Małecki, P.; Ablialimov, O.; Trzybiński, D.; Woźniak, K.; Osella, S.; Trzaskowski, B.; Grela, K. Azoliniums, adducts, NHCs and azomethine ylides: Divergence in Wanzlick equilibrium and olefin metathesis catalyst formation. *Chemistry* **2018**, *24*, 4785–4789. [[CrossRef](#)]
36. Blum, A.P.; Ritter, T.; Grubbs, R.H. Synthesis of *N*-heterocyclic carbene-containing metal complexes from 2-(pentafluorophenyl)imidazolidines. *Organometallics* **2007**, *26*, 2122–2124. [[CrossRef](#)]
37. Nyce, G.W.; Csihony, S.; Waymouth, R.M.; Hedrick, J.L. A general and versatile approach to thermally generated *n*-heterocyclic carbenes. *Chemistry* **2004**, *10*, 4073–4079. [[CrossRef](#)]
38. Addison, A.W.; Rao, T.N.; Reedijk, J.; van Rijn, J.; Verschoor, G.C. Synthesis, structure, and spectroscopic properties of copper(II) compounds containing nitrogen–sulphur donor ligands; the crystal and molecular structure of aqua[1,7-bis(*N*-methylbenzimidazol-2'-yl)-2,6-dithiaheptane]copper(II) perchlorate. *J. Chem. Soc. Dalton Trans.* **1984**, 1349–1356. [[CrossRef](#)]
39. Barbasiewicz, M.; Bieniek, M.; Michrowska, A.; Szadkowska, A.; Makal, A.; Woźniak, K.; Grela, K. Probing of the ligand anatomy: Effects of the chelating alkoxy ligand modifications on the structure and catalytic activity of ruthenium carbene complexes. *Adv. Synth. Catal.* **2007**, *349*, 193–203. [[CrossRef](#)]
40. Ledoux, N.; Linden, A.; Allaert, B.; Mierde, H.V.; Verpoort, F. Comparative investigation of Hoveyda–Grubbs catalysts bearing modified *N*-heterocyclic carbene ligands. *Adv. Synth. Catal.* **2007**, *349*, 1692–1700. [[CrossRef](#)]
41. Endo, K.; Herbert, M.B.; Grubbs, R.H. Investigations into ruthenium metathesis catalysts with six-membered chelating NHC ligands: Relationship between catalyst structure and stereoselectivity. *Organometallics* **2013**, *32*, 5128–5135. [[CrossRef](#)]
42. Lehman, S.E.; Wagener, K.B. Synthesis of ruthenium olefin metathesis catalysts with linear alkyl carbene complexes. *Organometallics* **2005**, *24*, 1477–1482. [[CrossRef](#)]
43. Samojłowicz, C.; Bieniek, M.; Pazio, A.; Makal, A.; Woźniak, K.; Poater, A.; Cavallo, L.; Wójcik, J.; Zdanowski, K.; Grela, K. The doping effect of fluorinated aromatic solvents on the rate of ruthenium-catalysed olefin metathesis. *Chemistry* **2011**, *17*, 12981–12993. [[CrossRef](#)]
44. Clavier, H.; Urbina-Blanco, C.A.; Nolan, S.P. Indenylidene ruthenium complex bearing a sterically demanding NHC ligand: An efficient catalyst for olefin metathesis at room temperature. *Organometallics* **2009**, *28*, 2848–2854. [[CrossRef](#)]
45. Yu, B.; Hamad, F.B.; Sels, B.; Van Hecke, K.; Verpoort, F. Ruthenium indenylidene complexes bearing *N*-alkyl/*N*-mesityl-substituted *N*-heterocyclic carbene ligands. *Dalton Trans.* **2015**, *44*, 11835–11842. [[CrossRef](#)] [[PubMed](#)]
46. Yu, B.; Li, Y.; He, X.; Hamad, F.B.; Ding, F.; Van Hecke, K.; Yusubov, M.S.; Verpoort, F. SIMes/PCy₃ mixed ligand-coordinated alkyl group-tagged ruthenium indenylidene complexes: Synthesis, characterization and metathesis activity. *Appl. Organomet. Chem.* **2018**, *32*, e4548. [[CrossRef](#)]
47. Vehlou, K.; Maechling, S.; Blechert, S. Ruthenium metathesis catalysts with saturated unsymmetrical *N*-heterocyclic carbene ligands. *Organometallics* **2006**, *25*, 25–28. [[CrossRef](#)]
48. Dąbrowski, M.; Wyřebek, P.; Trzybiński, D.; Woźniak, K.; Grela, K. In a quest for selectivity paired with activity: A ruthenium olefin metathesis catalyst bearing an unsymmetrical phenanthrene-based *N*-heterocyclic carbene. *Chemistry* **2020**, *26*, 3782–3794. [[CrossRef](#)]
49. Chatterjee, A.K.; Choi, T.-L.; Sanders, D.P.; Grubbs, R.H. A general model for selectivity in olefin cross metathesis. *J. Am. Chem. Soc.* **2003**, *125*, 11360–11370. [[CrossRef](#)] [[PubMed](#)]
50. Olszewski, T.K.; Bieniek, M.; Skowerski, K.; Grela, K. A new tool in the toolbox: Electron-withdrawing group activated ruthenium catalysts for olefin metathesis. *Synlett* **2013**, *24*, 903–919. [[CrossRef](#)]
51. Schmid, T.E.; Dumas, A.; Colombel-Rouen, S.; Crévisy, C.; Baslé, O.; Mauduit, M. From environmentally friendly reusable ionic-tagged ruthenium-based complexes to industrially relevant homogeneous catalysts: Toward a sustainable olefin metathesis. *Synlett* **2017**, *28*, 773–798.

52. Smoleń, M.; Marczyk, A.; Kośnik, W.; Trzaskowski, B.; Kajetanowicz, A.; Grela, K. Ruthenium-catalysed olefin metathesis in environmentally friendly solvents: 2-methyltetrahydrofuran revisited. *Eur. J. Org. Chem.* **2019**, *2019*, 640–646. [[CrossRef](#)]
53. Du Toit, J.I.; van der Gryp, P.; Looock, M.M.; Tole, T.T.; Marx, S.; Jordaan, J.H.L.; Vosloo, H.C.M. Industrial viability of homogeneous olefin metathesis: Beneficiation of linear alpha olefins with the diphenyl-substituted pyridinyl alcoholato ruthenium carbene precatalyst. *Catal. Today* **2016**, *275*, 191–200. [[CrossRef](#)]
54. Du Toit, J.I.; Jordaan, M.; Huijsmans, C.A.A.; Jordaan, J.H.L.; Van Sittert, C.G.C.E.; Vosloo, H.C.M. Improved metathesis lifetime: Chelating pyridinyl-alcoholato ligands in the second generation Grubbs precatalyst. *Molecules* **2014**, *19*, 5522–5537. [[CrossRef](#)]
55. Interestingly, the amount of isomerization products did not seem to decrease with the decrease in the ruthenium concentration. This results seems interesting in the light of recent publication of Fogg [See: Ref. [56]].
56. Nascimento, D.L.; Fogg, D.E. Origin of the breakthrough productivity of ruthenium–cyclic alkyl amino carbene catalysts in olefin metathesis. *J. Am. Chem. Soc.* **2019**, *141*, 19236–19240. [[CrossRef](#)]
57. Bailey, G.A.; Foscatto, M.; Higman, C.S.; Day, C.S.; Jensen, V.R.; Fogg, D.E. Bimolecular coupling as a vector for decomposition of fast-initiating olefin metathesis catalysts. *J. Am. Chem. Soc.* **2018**, *140*, 6931–6944. [[CrossRef](#)]
58. Bidange, J.; Dubois, J.-L.; Couturier, J.-L.; Fischmeister, C.; Bruneau, C. Ruthenium catalyzed ethenolysis of renewable oleonitrile. *Eur. J. Lipid Sci. Technol.* **2014**, *116*, 1583–1589. [[CrossRef](#)]
59. Alexander, K.A.; Paulhus, E.A.; Lazarus, G.M.L.; Leadbeater, N.E. Exploring the reactivity of a ruthenium complex in the metathesis of biorenewable feedstocks to generate value-added chemicals. *J. Organomet. Chem.* **2016**, *812*, 74–80. [[CrossRef](#)]
60. Bidange, J.; Fischmeister, C.; Bruneau, C. Ethenolysis: A green catalytic tool to cleave carbon–carbon double bonds. *Chemistry* **2016**, *22*, 12226–12244. [[CrossRef](#)]
61. Marx, V.M.; Sullivan, A.H.; Melaimi, M.; Virgil, S.C.; Keitz, B.K.; Weinberger, D.S.; Bertrand, G.; Grubbs, R.H. Cyclic alkyl amino carbene (CAAC) ruthenium complexes as remarkably active catalysts for ethenolysis. *Angew. Chem. Int. Ed.* **2015**, *54*, 1919–1923. [[CrossRef](#)]
62. Gawin, R.; Kozakiewicz, A.; Guńka, P.A.; Dąbrowski, P.; Skowerski, K. Bis(cyclic alkyl amino carbene) ruthenium complexes: A versatile, highly efficient tool for olefin metathesis. *Angew. Chem. Int. Ed.* **2017**, *56*, 981–986. [[CrossRef](#)]
63. Kajetanowicz, A.; Chwalba, M.; Gawin, A.; Tracz, A.; Grela, K. Non-glovebox ethenolysis of ethyl oleate and fame at larger scale utilizing a cyclic (alkyl)(amino)carbene ruthenium catalyst. *Eur. J. Lipid Sci. Technol.* **2020**, *122*, 1900263. [[CrossRef](#)]
64. Engl, P.S.; Santiago, C.B.; Gordon, C.P.; Liao, W.-C.; Fedorov, A.; Copéret, C.; Sigman, M.S.; Togni, A. Exploiting and understanding the selectivity of Ru-*N*-heterocyclic carbene metathesis catalysts for the ethenolysis of cyclic olefins to α,ω -dienes. *J. Am. Chem. Soc.* **2017**, *139*, 13117–13125. [[CrossRef](#)]

